2005 American Control Conference
June 8-10, 2005. Portland, OR, USA

Voltage Regulation in Series Resonant DC-to-DC Power Converters with unknown Resistive Load

V. M. Hernández, G. Herrera and B. Zúñiga

Universidad Autónoma de Querétaro. Facultad de Ingeniería.
Apartado Postal 3-24. C.P. 76150, Querétaro, Qro., México.
Phone: + 52 (442) 1 92 12 64, ext. 258, ext. 103 (Fax).
vmhg@uaq.mx

Abstract— **In this note we present a control strategy combining continuous and discrete time control schemes to regulate the average voltage at the load in series resonant DC-to-DC power converters. We succeed to regulate, at a constant desired value, the average voltage in the resistive load in spite of the unknown load and uncertain values of the DC power supply. The design of the discrete time part of the controller relies on static nonlinearities satisfying a sector condition.**

I. INTRODUCTION.

Along the last years DC-to-DC power conversion based on solid state switching devices has been very important in reducing the size of actual electronic equipment. Further, the large number of portable electronic equipment in every day's life would not be possible without actual DC-to-DC power converters based on semiconductor switching devices. However, from the control point of view lots of work rest to be done. This is particularly true in the case of resonant DC-to-DC power converters which are studied in this note. The aim of these converters is, given a DC power supply, to produce a desired DC voltage at the load which is different from voltage of the DC power supply. Resonant DC-to-DC power converters are strongly nonlinear because of the inherently discrete character of its input, generated by means of switching power devices. The traditional method for control design in these devices consists in linear approximations based on harmonic analysis [3]. Motivated by the obvious limitations of this method, several new approaches have been introduced recently (see [5],[6] and references there in). In particular, the paper [6] presents two controllers for series resonant DC-to-DC power converters using the hybrid flatness property of the model. Remarkable is the fact that no approximations are used. The first controller is intended to induce a resonant behavior in the circuit although the average voltage at the load cannot be modified. A complete stability and robustness analysis as well as computation of the ripple voltage was presented in [1] for this controller. In the second controller a new switching surface is introduced which can be specified by means of a design parameter represented by k. Hence, different values of the average voltage at the load can be obtained by selecting a different value of k. However, several issues remain to be studied: no method is presented to compute a priori the average voltage at the load, further this average voltage is strongly affected by changes in both the load and the supplied DC voltage. It is clear that these problems are important obstacles for practical applications. In this note, we present a discrete-time integral law which, combined with the second controller proposed in [6], succeeds to eliminate the fore mentioned disadvantages, which represents our main contribution. Its is worth mentioning that in [6] convergence to the induced limit cycle is not proven rigorously but only by means of simulations and experiments. Further, no stability analysis is presented. Hence, we present a modest advancement in this direction by proving that the state is bounded when the second control scheme presented in [6] is used. Thus, assuming asymptotic convergence to the limit cycle induced by this controller we do prove that use of the combined continuous-discrete time controller achieves asymptotic convergence of the average voltage at the load to its desired constant value. Further, the domain of convergence can be enlarged arbitrarily by means of a suitable choice of the controller parameters. The stability analysis relies on the fact that use of the controller proposed in [6] allows that, after some transient period, the average voltage at the load and the parameter k of this controller are related through a static nonlinearity satisfying some sector condition. Thus, the sampling period used in the discrete-time part of the controller must be selected large enough to allow that such transient period has finished. It is worth mentioning that a similar control strategy has been proposed recently by the authors for series resonant inverters in [2]. This note is organized as follows. In section II the dynamic model we consider is presented. Section III is devoted to explain the system response. In section IV we present a Lyapunov based analysis to prove that the state is bounded when the second controller in [6] is used. In section V we study the relation, in stationary state, between the average voltage at the load and parameter k of controller [6]. We present our main contribution in section VI. Finally, we present some simulation results in section VII and some concluding remarks in section VIII.

II. The dynamic model considered.

This section is entirely based on the results reported in [6][5]. The electric circuit of a series resonant DC-to-DC power converter is presented in fig. 1. The corresponding dynamic model is given as:

$$L\frac{di}{dt} = -v - v_0 sign(i) + E(t) \qquad (1)$$

$$C\frac{dv}{dt} = i, \quad C_0\frac{dv_0}{dt} = abs(i) - \frac{v_0}{R} \qquad (2)$$

where $sign(\cdot)$ represents the sign function defined as:

$$sign(x) = \begin{cases} 1, & x \geq 0 \\ -1, & x < 0 \end{cases} \qquad (3)$$

$abs(\cdot)$ stands for the absolute value function, L and C are, respectively, the resonant inductance and capacitance, C_0 is the filtering capacitance, R is the load resistance, i and v are, respectively, the resonant electric current and voltage, v_0 is voltage at the load and $E(t)$ stands for the input voltage which can only take two discrete values $\{+E, -E\}$, where E is the constant voltage of the DC power supply. Consider the following coordinate change:

$$z_1 = \frac{i}{E}\sqrt{\frac{L}{C}},\ z_2 = \frac{v}{E},\ z_3 = \frac{v_0}{E},\ \tau = \frac{t}{\sqrt{LC}} \qquad (4)$$

Thus, the following normalized model is obtained:

$$\dot{z}_1 = -z_2 - z_3 sign(z_1) + \delta\, u \qquad (5)$$

$$\dot{z}_2 = z_1 \qquad (6)$$

$$\alpha\dot{z}_3 = abs(z_1) - \frac{z_3}{Q} \qquad (7)$$

where, with some abuse of notation, the " $\cdot$ " represents the derivative with respect to the normalized time τ. The variable u is the normalized input variable restricted to take only two values $\{-1, +1\}$ and $\delta = 1$ if the DC power supply delivers its nominal voltage, i.e. E, otherwise $\delta \neq 1$. We define parameters $Q = R\sqrt{C/L}$ and $\alpha = C_0/C$. Note that Q^{-1} is known as the *quality factor* of the series resonant converter. We stress that normal values are such that $\alpha \gg 1$, to keep small the ripple voltage at the load, and $Q^{-1} > 2.5$, to ensure the circuit to oscillate [3], and $\alpha > Q^{-1}$. Based in the flatness properties of model (5), (6), (7) the following control law is proposed to control the average voltage at the load:

$$u = sign(\sigma), \qquad \sigma = z_1 - k\, z_2, \quad k \geq 0 \qquad (8)$$

III. System response.

In what follows we assume that no uncertainty is present in the supplied DC voltage E, i.e. $\delta = 1$. We will study in section V the case when the supplied DC voltage E is not exactly known, i.e. $\delta \neq 1$. It is not difficult to see that use of control law (8) in (5), (6), (7) yields a hybrid piecewise linear system which is defined in four different regions:

1) $z_1 < 0$, $\sigma > 0$:

$$\begin{pmatrix} \dot{z}_1 \\ \dot{z}_2 \\ \dot{z}_3 \end{pmatrix} = \begin{pmatrix} 0 & -1 & 1 \\ 1 & 0 & 0 \\ \frac{-1}{\alpha} & 0 & \frac{-1}{\alpha Q} \end{pmatrix} \begin{pmatrix} z_1 \\ z_2 \\ z_3 \end{pmatrix} + \begin{pmatrix} 1 \\ 0 \\ 0 \end{pmatrix} \qquad (9)$$

2) $z_1 > 0$, $\sigma > 0$:

$$\begin{pmatrix} \dot{z}_1 \\ \dot{z}_2 \\ \dot{z}_3 \end{pmatrix} = \begin{pmatrix} 0 & -1 & -1 \\ 1 & 0 & 0 \\ \frac{1}{\alpha} & 0 & \frac{-1}{\alpha Q} \end{pmatrix} \begin{pmatrix} z_1 \\ z_2 \\ z_3 \end{pmatrix} + \begin{pmatrix} 1 \\ 0 \\ 0 \end{pmatrix} \qquad (10)$$

3) $z_1 > 0$, $\sigma < 0$:

$$\begin{pmatrix} \dot{z}_1 \\ \dot{z}_2 \\ \dot{z}_3 \end{pmatrix} = \begin{pmatrix} 0 & -1 & -1 \\ 1 & 0 & 0 \\ \frac{1}{\alpha} & 0 & \frac{-1}{\alpha Q} \end{pmatrix} \begin{pmatrix} z_1 \\ z_2 \\ z_3 \end{pmatrix} - \begin{pmatrix} 1 \\ 0 \\ 0 \end{pmatrix} \qquad (11)$$

4) $z_1 < 0$, $\sigma < 0$:

$$\begin{pmatrix} \dot{z}_1 \\ \dot{z}_2 \\ \dot{z}_3 \end{pmatrix} = \begin{pmatrix} 0 & -1 & 1 \\ 1 & 0 & 0 \\ \frac{-1}{\alpha} & 0 & \frac{-1}{\alpha Q} \end{pmatrix} \begin{pmatrix} z_1 \\ z_2 \\ z_3 \end{pmatrix} - \begin{pmatrix} 1 \\ 0 \\ 0 \end{pmatrix} \qquad (12)$$

It is easy to verify that, for any $k \geq 0$: $i)$ the equilibrium point of systems defined in regions $1)$ and $2)$ is $(z_1, z_2, z_3) = (0, 1, 0)$, which does not belong to any of these regions (see fig. 3), and $ii)$ the equilibrium point of systems defined in regions $3)$ and $4)$ is $(z_1, z_2, z_3) = (0, -1, 0)$, which does not belong to any of these regions. Hence, system evolution is always far from its equilibrium points. Note that this is not the case when $k < 0$. On the other hand, it is not difficult to show that systems given in (9), (10), (11) and (12) are the same when $k < 0$, i.e., all of them define linear exponentially stable systems. Hence, for some initial conditions the state evolution in each region converges to either $(z_1, z_2, z_3) = (0, 1, 0)$ or $(z_1, z_2, z_3) = (0, -1, 0)$. Because of this, aside from some values of k close to zero, do not exist any limit cycle for $k < 0$. This represents a strong justification to use $k \geq 0$ in the control law (8).

Solving the piecewise linear system in each region ($k \geq 0$) we can obtain analytically the hybrid system response by concatenating the solution in adjacent regions. Hence, by increasing time from zero we find that the state converges to a limit cycle. Further, as shown in [6][5] through simulations and experiments, if L, C, C_0 are kept constant the location of this limit cycle only depends on k and Q, i.e., the controller switching surface and the load. However, the analytical solution depends on k and Q in a very complicated manner and, because of that, it is very difficult to obtain an analytical expression relating the final average value of voltage at the load and parameters k and Q. Hence, it is difficult to determine the value of k required to obtain the desired voltage at the load, even if Q is known. On the other hand, computation of the Poincaré map eigenvalues as done in [1] is useless to determine the limit cycle stability properties. The main reason can be explained as follows. According to the piecewise linear character of the closed loop system, we have to use the boundaries of regions 1), 2), 3) and 4) as the cross-sections required to construct the Poincaré map [7]. Although the limit cycle is periodic, however, for any slight deviation of the state from the limit cycle the flight time is not constant in each particular region as long as the limit cycle is not reached. This is different from the situation in [1] where, due to the combined existence of a unique cross-section $z_1 = 0$ and the resonant behavior of the circuit, the flight time is always constant whether the state is located on the limit cycle or not. The direct consequence in the present case of study is that the resulting (linear discrete-time two-dimensional) Poincaré map has a matrix with one eigenvalue outside the unit circle, i.e., the limit cycle seems to be unstable. However, as explained above, the system evolution can be computed to find that the state does converge to the limit cycle. In spite of this apparent contradiction none of these results are wrong:

First we recall that, as explained above, the flight time is not constant outside the limit cycle. If we select as initial condition a point that does not belong to the limit cycle but does belong to either $z_1 = 0$ or $\sigma = 0$ and we sample with the period of the limit cycle then we would find that the discrete-time state does converges to one point belonging to the limit cycle but not belonging to any of the surfaces $z_1 = 0$ or $\sigma = 0$. Thus, according to the Poincaré map the discrete-time state leaves the equilibrium point defined on either $z_1 = 0$ or $\sigma = 0$ and goes elsewhere, i.e. the equilibrium point is unstable, although the continuous-time state does converges asymptotically to the limit cycle.

Although asymptotic stability of this limit cycle is not proven, because of these difficulties, however in the next section we succeed to prove some stability properties.

IV. Boundedness of the state.

Consider the following positive definite, radially unbounded function:

$$V(z_1, z_2, z_3) = \frac{1}{2}z_1^2 + \frac{1}{2}z_2^2 + \frac{1}{2}z_3^2 \tag{13}$$

whose time derivative along the trajectories of (5), (6), (7) is given as:

$$\begin{aligned} \dot{V} &= z_1\left[-z_2 - z_3 sign(z_1) + u\right] + z_2 z_1 + \\ &+ z_3\left[abs(z_1) - \frac{z_3}{Q}\right] 1/\alpha \end{aligned} \tag{14}$$

Using (8) we can write this time derivative in each of the fore mentioned regions as:

1) $z_1 < 0$, $\sigma > 0$: $\dot{V} = z_1 + z_3 z_1(1 - 1/\alpha) - \frac{z_3^2}{\alpha Q}$
2) $z_1 > 0$, $\sigma > 0$: $\dot{V} = z_1 - z_3 z_1(1 - 1/\alpha) - \frac{z_3^2}{\alpha Q}$
3) $z_1 > 0$, $\sigma < 0$: $\dot{V} = -z_1 - z_3 z_1(1 - 1/\alpha) - \frac{z_3^2}{\alpha Q}$
4) $z_1 < 0$, $\sigma < 0$: $\dot{V} = -z_1 + z_3 z_1(1 - 1/\alpha) - \frac{z_3^2}{\alpha Q}$

We recall that $0 < 1/\alpha \ll 1$, $Q^{-1} > 2.5$ and $z_3 \geq 0$ for a normal operation of the circuit. According to this:

1) $z_1 < 0$, $\sigma > 0$:

$$\begin{aligned} \dot{V} &< 0, \qquad z_1 \neq 0 \; or \; z_3 \neq 0, \\ \dot{V} &= 0, \qquad z_1 = z_3 = 0 \end{aligned} \tag{15}$$

2) $z_1 > 0$, $\sigma > 0$:

$$\dot{V} < 0, \quad z_3 > \frac{1}{1 - 1/\alpha} > 0 \tag{16}$$

3) $z_1 > 0$, $\sigma < 0$:

$$\begin{aligned} \dot{V} &< 0, \qquad z_1 \neq 0 \; or \; z_3 \neq 0, \\ \dot{V} &= 0, \qquad z_1 = z_3 = 0 \end{aligned} \tag{17}$$

4) $z_1 < 0$, $\sigma < 0$:

$$\dot{V} < 0, \quad z_3 > \frac{1}{1 - 1/\alpha} > 0 \tag{18}$$

This means that z_3 is bounded because of the radial unboundedness of V. On the other hand, we remark that z_3 is the response of the first order asymptotically stable linear system:

$$\dot{z}_3 + \frac{1}{\alpha Q} z_3 = \frac{1}{\alpha}\mu(\tau) \tag{19}$$

where $\mu(\tau) = abs(z_1(\tau))$. Hence, large values of z_3 are due to either $i)$ large initial values of z_3, hence, due to the asymptotic stability properties of (19), z_3 will decrease to values which can be sustained by $abs(z_1)$, or $ii)$ large values of z_1. Suppose that z_3 is small and $abs(z_2)$ is so large that we can approximate (5) by $\dot{z}_1 = -z_2$. This means that (5) and (6) become an harmonic oscillator and, hence, large values of z_2 imply large values of z_1 (in the case that both z_3 and $abs(z_2)$ are large, the approximation $\dot{z}_1 = -z_2$ may not stand, but in such a case $\dot{V} < 0$, i.e. (15)-(18), and the whole state would be bounded). Now, because of the dynamics of (19), although z_1 may be large whereas z_3 is small, however this is possible only during short periods of time determined by the time constant αQ of (19), and because of the linearity of the system in each region neither z_1 or z_2 have finite scape time. This means that, excepting short periods of time, z_1 and z_2 are large only if z_3 is large. Thus, recalling that $\dot{V} < 0$ if z_3 is large enough, we conclude that $\dot{V} < 0$ for $\|z_1, z_2, z_3\|_2$ large enough, where $\|\cdot\|_2$ represents the Euclidean norm. Thus, invoking the radial unboundedness of V, this ensures boundedness of the whole state.

V. Dependence of z_3 on k and Q.

In spite of the lack of any asymptotic stability proof, we know that z_3 converges to an oscillatory function whose average value, $\bar{z}_3$, is positive. As explained in section III, this can be seen by computing the analytical response of the hybrid system and was also found in [6][5] through simulations and experiments. Unfortunately, as shown in

[6][5], this average value is affected by the load Q and by uncertainties on the DC power supply voltage, i.e δ defined in section II. In practice it is of prime interest to supply a prescribed voltage at the load without any a priori knowledge of the actual load Q and in spite of uncertainties on the supplied DC voltage. We solve these problems in the following section. On the other hand, controller (8) allows to modify the average voltage at the load $\bar{z}_3$ by using different values of the controller parameter k. However, we recall that is very complicated to find an analytical relation between $\bar{z}_3$ and k. Hence, in what follows we use simulations. In fig. 4a) we present some simulation results where we can see that $\bar{z}_3$ is given as inverse like functions of k parameterized by the load Q (i.e., R) which entirely lay on the first quadrant in the $\bar{z}_3 - k$ plane.

Remark 1: A similar conclusion can be obtained as follows. First note that the dynamics of z_3 is slow compared with the dynamics of z_2 and z_3 because $\alpha \gg 1$ in (19). This means that we can consider that z_3 remains approximately constant during the time it takes to z_1 and z_2 to complete a oscillating cycle. Now note that, in general terms, for any $k > 0$ the time that it takes to the system to travel though regions $2)$ and $4)$ is larger than the time that it takes to the system to travel through regions $1)$ and $3)$. This can be roughly seen from the size of the space corresponding to each region in fig. 3. Also note that in the latter regions the energy of the whole system always decreases (see (15), (17)). On the other hand, we can see that in regions $2)$ and $4)$ the energy of the system increases if z_3 is small. Further because of the fore mentioned property on the time spent by the system in each region we conclude that, for small values of z_3 the energy of the system increases, although not monotonically, but in an oscillatory manner. Note that: $a)$ for larger values of k the difference between the fore mentioned times spent in each region decreases (see fig. 3) and, $b)$ for large values of z_3 the increment of energy in regions $2)$ and $4)$ is smaller and smaller until it becomes a decrement of energy. These facts mean that, for larger values of k an equilibrium between increments and decrements of the total energy of the system is obtained for smaller values of z_3, i.e. for larger $k > 0$ we have that $\bar{z}_3$ is smaller. Thus, a dependence between $\bar{z}_3$ and k is expected to be similar to that shown in fig. 4

In fig. 4b) we present simulation results for different values of δ when Q is kept constant ($R = 72\Omega$). We can see that, similarly to results in fig. 4a), $\bar{z}_3$ are inverse like functions of k, parameterized by δ, laying in the first quadrant. This information, given in fig. 4 a) and b), is enough to design the controller that we present in the following section.

VI. INTEGRAL CONTROL OF $\bar{z}_3$.

We assume that the closed loop system (5), (6), (7), (8) converges asymptotically to a limit cycle such that the average voltage at the load $\bar{z}_3$ is modified by the controller parameter k, and affected by δ, according to last section. This is the core of the design we present below. The average voltage $\bar{z}_3$ is obtained at the load after a transient period which may take several hundreds of normalized units of time. We propose to adjust the value of k when such transient period has finished, i.e., we use a discrete time control law to rule the adjustments in k. The following discrete-time law is proposed:

$$k = \gamma G(z)(\bar{z}_3 - \bar{z}_{3d}) \tag{20}$$

where:

$$G(z) = \frac{z^{-1}T}{1 - z^{-1}} \tag{21}$$

$\gamma > 0$ is a constant to be determined, z represents the Z-transform variable and T is the sampling period which is selected to be large enough to ensure that a stationary response is obtained in the closed loop system (5), (6), (7), (8). According to the previous section, selecting T under this criterion allows us to treat the whole closed loop dynamical system (5), (6), (7), (8) as a static nonlinearity $\varphi(k) = \bar{z}_3$ having a inverse like shape. Hence, we can use some manipulations to obtain the block diagram shown in fig. 2, where $y = k - k_d$, $\chi = e = \bar{z}_{3d} - \bar{z}_3$ and k_d represents the value of k necessary to obtain the desired average voltage at the load $\bar{z}_{3d}$. We can see that the static nonlinearity $\chi(y)$ satisfies the sector condition [4]:

$$(\chi - \alpha\, y)(\chi - \beta\, y) \leq 0 \tag{22}$$

for some $\beta > \alpha > 0$, in a finite domain $y \in [-a, b]$ for some $a > 0$, $b > 0$. Consider the following Lyapunov function candidate:

$$W(y(\kappa)) = p\, y^2(\kappa) \tag{23}$$

where $p > 0$ is a constant and κ represents the discretized time. We can use (20), (21) to write:

$$y(\kappa + 1) = -\gamma T e(\kappa) + y(\kappa) \tag{24}$$

Using this we have the following:

$$\begin{aligned} & W(y(\kappa+1)) - W(y(\kappa)) = \\ = \quad & -pe(\kappa)T\gamma[-e(\kappa)T\gamma + 2\, y(\kappa)] \end{aligned} \tag{25}$$

Now, consider some $\eta > 0$, hence:

$$\begin{aligned} & W(y(\kappa+1)) - W(y(\kappa)) \leq \\ \leq \quad & -e(\kappa)T\gamma p[-e(\kappa)T\gamma + 2\, y(\kappa)] + \eta y^2(\kappa) \\ = \quad & \chi^2(\kappa)(T\gamma)^2 p - 2pT\gamma\, y(\kappa)\chi(\kappa) + \eta y^2(\kappa) \end{aligned} \tag{26}$$

Define $p = \frac{1}{(T\gamma)^2}$ hence:

$$\begin{aligned} & W(y(\kappa+1)) - W(y(\kappa)) \leq \\ \leq \quad & \chi^2(\kappa) - \frac{2}{T\gamma}\chi(\kappa)\, y(\kappa) + \eta y^2(\kappa) \end{aligned} \tag{27}$$

Recall the sector condition (22):

$$\begin{aligned} & \chi^2(\kappa) - (\alpha + \beta)\, y(\kappa)\chi(\kappa) + \alpha\beta\, y^2(\kappa) = \\ = \quad & [\chi(\kappa) - \alpha\, y(\kappa)][\chi(\kappa) - \beta\, y(\kappa)] \leq 0 \end{aligned} \tag{28}$$

Suppose that

$$\begin{aligned}&\chi^2(\kappa)-\frac{2}{T\gamma}\chi(\kappa)\,y(\kappa)+\eta y^2(\kappa)=\\ =\ &\chi^2(\kappa)-(\alpha+\beta)\,y(\kappa)\chi(\kappa)+\alpha\beta\,y^2(\kappa)\end{aligned}\tag{29}$$

hence:

$$\begin{aligned}W(y(\kappa+1))-W(y(\kappa)) &< 0,\ y(\kappa)\neq 0,\ \chi(\kappa)\neq 0\\ W(y(\kappa+1))-W(y(\kappa)) &= 0,\ y(\kappa)=0,\ \chi(\kappa)=0\end{aligned}$$

We stress that according to the sector condition either $[\chi(\kappa)-\alpha\ y(\kappa)]=0$ or $[\chi(\kappa)-\beta\ y(\kappa)]=0$ imply both $y=0$ and $e=0$ in the finite domain $y\in[-a,b]$. Thus, asymptotic stability of the equilibrium point $\bar z_3=\bar z_{3d}$ is ensured. On the other hand, (29) is true if and only if:

$$\alpha+\beta=\frac{2}{T\gamma},\qquad \alpha\beta=\eta\tag{30}$$

hence:

$$\beta^2-\frac{2}{T\gamma}\beta+\eta\ =\ 0\tag{31}$$

Solving this quadratic equation:

$$\begin{aligned}\beta &= \frac{1}{T\gamma}+\sqrt{\frac{1}{(T\gamma)^2}-\eta}\\ \alpha &= \frac{\eta}{\beta},\qquad 0<\eta<\frac{1}{(T\gamma)^2}\end{aligned}\tag{32}$$

If we choose η to be closer to zero then $\beta<\frac{2}{T\gamma}$ will be larger and $\alpha>0$ closer to zero. Further, if we choose $\gamma\to 0$ then $\frac{2}{T\gamma}\to\infty$. Hence, β can be done larger and α smaller by a suitable selection of the controller parameter γ, i.e., the domain $y\in[-a,b]$ can be enlarged arbitrarily. This completes the proof of the following proposition.

Proposition 1: Assume that the closed loop system (5), (6), (7), (8) achieves asymptotic convergence of the average voltage at the load, $\bar z_3$, to $\varphi(k)$, i.e. an inverse like function of parameter k. Let $\bar z_{3d}$ and k_d be, respectively, the desired value of the average voltage at the load and the value of the controller parameter k necessary to achieve $\bar z_3=\bar z_{3d}$. Let k_d be computed using the discrete-time adjusting rule (20), (21) where the sampling period T is selected according to the reasoning presented in the paragraph after (21) and $\gamma>0$ is a constant chosen in such a way that given a constant $0<\eta<\frac{1}{(T\gamma)^2}$ there exist two positive constants α and β, $\alpha<\beta$ satisfying (32) and the sector condition (22) in some finite domain $y\in[-a,b]$, for some $a>0,\ b>0$. Then $\bar z_3$ converges to $\bar z_{3d}$ in the domain $y\in[-a,b]$ and the whole state $[z_1,z_2,z_3]^T$ remains bounded. Further, the domain $y\in[-a,b]$ can be enlarged arbitrarily by choosing the controller parameter $\gamma\to 0$.

Remark 2: Note that this control strategy achieves $\bar z_3\to\bar z_{3d}$ without exact information about the resistive load and in spite of uncertainties on the voltage of the DC power supply. On the other hand, although asymptotic convergence $\bar z_3\to\varphi(k)$ means that $\bar z_3=\varphi(k)$ is true only after an infinite period of time, however sector condition (22) introduces nice robustness properties that allow to activate the discrete-time adjusting rule (20), (21) just after a finite period of time.

Remark 3: We stress that although choosing $\gamma\to 0$ enlarges the domain $y\in[-a,b]$, however such a selection of γ degrades progressively the closed loop performance. Note, however, that this is a common feature in controllers claiming semiglobal asymptotic stability.

VII. Simulation results.

In simulations we used the numerical values proposed in [6], i.e.: $E=48$[V], $L=1.5\times10^{-3}$[H], $C=10.6\times10^{-9}$[F], $R=72[\Omega]$, i.e., $Q^{-1}=5.2247$ and $C_0=1\times10^{-6}$[F], i.e., $\alpha=94.34$. In all simulations we used the hybrid control law presented in proposition 1. Controller parameters were chosen to be $\gamma=95\times10^{-5}$, $T=400$, i.e, $\beta<5.26$, $\alpha>0$. We stress that the corresponding sampling period in the original time coordinates, t, is 1.595×10^{-3}[sec]. The desired average voltage was chosen to be $\bar z_{3d}=0.35$, i.e., the desired average voltage at the load in original coordinates is $\bar v_{0d}=16.8$[V]. We used $k(0)=1$ as the initial condition of the discrete-time system (20), (21). In fig. 5 we present simulations for three different cases: $a)$ $R=72[\Omega]$, $E=48$[V], $b)$ $R=35[\Omega]$, $E=48$[V], and $c)$ $R=72[\Omega]$, $E=35$[V], i.e. $\delta=0.729$. As we can see convergence of the average value of v_0 to $\bar v_{0d}$ (represented by a horizontal line) is obtained in all cases. We stress that this convergence is obtained without any knowledge of the resistive load and in spite of uncertainty in the voltage of the DC power supply. We also show, in fig. 5, the time evolution of parameter k. Note that different values of this parameter are necessary to compensate different loads and uncertainties in the supplied DC voltage.

VIII. Conclusions.

We have presented a strategy which combines continuous and discrete time control schemes for series resonant DC-to-DC power converters. The continuous time part of the controller was proposed recently and is based on flatness ideas. The discrete time part of the controller consists of a discrete time integral law. The latter is intended to adjust the unique parameter of the flatness based controller in such a way that the average voltage at the load converges to a preestablished constant desired value. We succeed to do this even if there are uncertainties in the constant supplied DC voltage and without any information on the actual resistive load. Existence of a limit cycle and its asymptotically stability has been shown through simulations and experiments in previous papers. Although we do not prove either the asymptotic stability of this limit cycle, however we do prove boundedness of the whole state. On the other hand, assuming asymptotic stability of the limit cycle we do prove asymptotic convergence, in a finite domain, of the average voltage at the load to its desired value when the combined control scheme is used. Further, this finite domain can be arbitrarily enlarged by means of suitable selection of the controller parameters.

REFERENCES

[1] Hernández V.M., Silva-Ortigoza R. and Sira-Ramírez H., "On the stability of limit cycles in resonant DC-to-DC power converters", *Proc. 42nd Conference on Decision and Control*, pp. 1141-1146, Maui, Hawaii, December 2003.

[2] Hernández V.M. and Silva-Ortigoza R., "Energy based control of series resonant inverters", *Proc. 43rd Conference on Decision and Control*, pp. 3515-3520, Bahamas, December, 2004.

[3] M. K. Kazimierczuk and D. Czarkowski. "Resonant Power Converters", *John Wiley and Sons Inc.*, New York, 1995.

[4] H. Khalil. "Nonlinear Systems", *Maxwell Macmillan Canada*, 1992.

[5] Silva-Ortigoza R., "Control de convertidores resonantes mediante planitud diferencial: Diseño y construcción" (in spanish) *M.Sc. Thesis, CINVESTAV*, México. February 2002.

[6] Sira-Ramírez H. and R. Silva-Ortigoza, "On the control of the resonant converters: a hybrid-Flatness Approach", *Proc. 15th International Symposium on Mathematical Theory of Networks and Systems*, South Bend, Indiana, August, 2002.

[7] Wiggins S., "Introduction to Applied Nonlinear Dynamical Systems and Chaos", *Springer-Verlag*, New York, 1990.

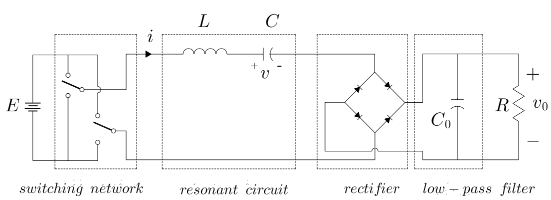

Fig. 1. Series resonant DC-to-DC power converter.

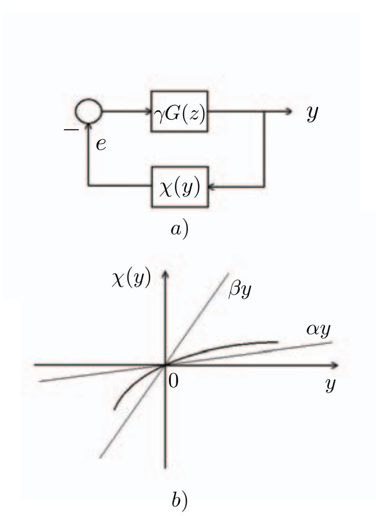

Fig. 2. a) Block diagram of the control strategy used to adjust k, b) Static nonlinearity.

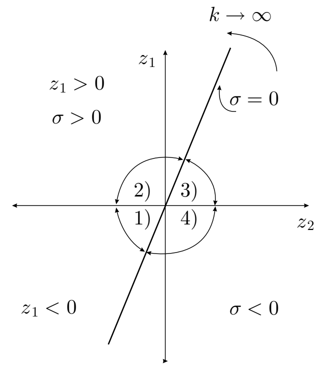

Fig. 3. Regions 1), 2), 3) and 4).

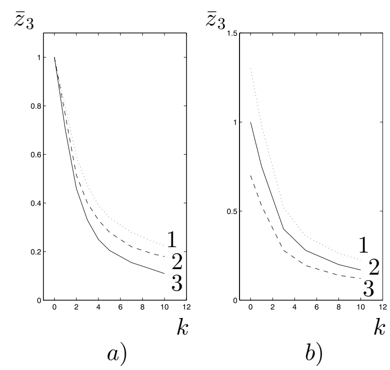

Fig. 4. a) $\bar{z}_3$ as a function of k: (1) $R = 150\Omega$, (2) $R = 72\Omega$, (3) $R = 10\Omega$, b) $\bar{z}_3$ as a function of k: (1) $\delta = 1.3$, (2) $\delta = 1$, (3) $\delta = 0.7$.

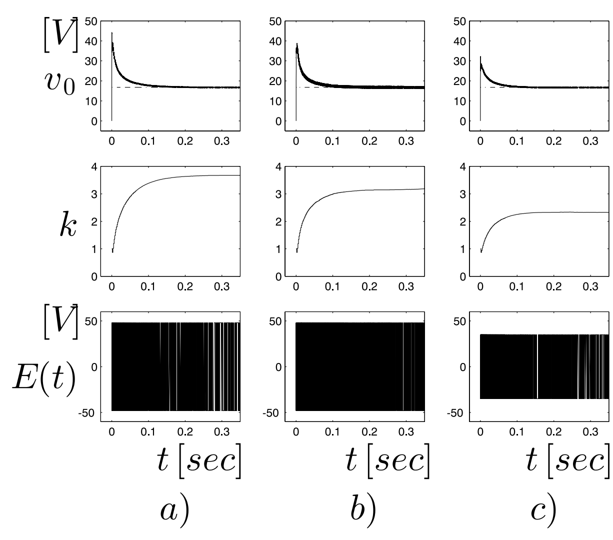

Fig. 5. Simulation results. a) $R = 72[\Omega]$, b) $R = 35[\Omega]$, c) $R = 72[\Omega]$ and $E = 35V$.